Title

Logical design of oral glucose ingestion pattern minimizing blood glucose in humans

Author

Masashi Fujii[1,2,*], Yohei Murakami[3,*], Yasuaki Karasawa[4,5,*], Yohei Sumitomo[2], Suguru Fujita[2], Masanori Koyama[6], Shinsuke Uda[7], Hiroyuki Kubota[7], Hiroshi Inoue[8], Katsumi Konishi[9], Shigeyuki Oba[3], Shin Ishii[3,10], Shinya Kuroda[1,2,10]

Lead Contact

Shinya Kuroda: skuroda@bs.s.u-tokyo.ac.jp

Affiliation

[1]Molecular Genetic Research Laboratory, Graduate School of Science, The University of Tokyo, Tokyo, 113-0033, Japan

[2]Department of Biological Sciences, Graduate School of Science, The University of Tokyo, Tokyo, 113-0033, Japan

[3]Department of Systems Science, Graduate School of Informatics, Kyoto University, Kyoto, 606-8501, Japan

[4]Department of Neurosurgery, The University of Tokyo Hospital

[5]Department of Rehabilitation, Graduate School of Medicine, The University of Tokyo,

113-0033, Japan

[6]Department of Mathematics, Graduate School of Science and Engineering, Ritsumeikan University, Shiga, 525-8577, Japan

[7]Division of Integrated Omics, Research Center for Transomics Medicine, Medical Institute of Bioregulation, Kyushu University, Fukuoka, 812-8582, Japan

[8]Metabolism and Nutrition Research Unit, Institute for Frontier Science Initiative, Kanazawa University, Ishikawa, 920-8640, Japan

[9]Department of Computer Science, Faculty of Informatics, Kogakuin University, Tokyo, 163-8677, Japan

[10]CREST, Japan Science and Technology Agency, Tokyo, 113-0033, Japan

[*]These authors contributed equally to this work.

SUMMARY

Excessive increase in blood glucose level after eating increases the risk of macroangiopathy, and a method for not increasing the postprandial blood glucose level is desired. However, a logical design method of the dietary ingestion pattern controlling the postprandial blood glucose

level has not yet been established. We constructed a mathematical model of blood glucose control by oral glucose ingestion in 3 healthy human subjects, used the model to predict an optimal glucose ingestion pattern, and showed that the optimal ingestion pattern minimized the peak value of blood glucose level. Subjects orally ingested 3 doses of glucose by bolus or over 2 hours, and blood glucose, insulin, C-peptide and incretins were measured for 4 hours. We constructed an ordinary differential equation model that reproduced the time course data of the blood glucose and blood hormone levels. Using the model, we predicted that intermittent ingestion 30 minutes apart was the optimal glucose ingestion patterns that minimized the peak value of blood glucose level. We confirmed with subjects that this intermittent pattern decreased the peak value of blood glucose level. This approach could be applied to design optimal dietary ingestion patterns.

In Brief

As a forward problem, we measured blood glucose and hormones in three human subjects after oral glucose ingestion and constructed a mathematical model of blood glucose control. As an inverse problem, we used the model to predict the optimal oral glucose ingestion pattern that minimized the peak value of blood glucose level, and validated the pattern with the subjects.

Highlights

- Modeling blood glucose concentrations predicts an intermittent ingestion pattern is optimal
- Human validation shows ingestion at 30-minute intervals limits peak blood glucose
- We provide a strategy to design optimal dietary ingestion patterns

INTRODUCTION

In healthy people, blood glucose levels are stably maintained and show only a slight postprandial increase (Abdul-Ghani et al., 2006). However, massive postprandial increases in blood glucose levels emerge in patients with the type 2 diabetic mellitus (T2DM) and impaired glucose tolerance (Edelstein et al., 1997). This postprandial hyperglycemia requires prevention and treatment, because it is associated with increased risk of cardiac and cerebrovascular complications (Nakagami and DECODA Study Group, 2004). Postprandial blood glucose originates from dietary carbohydrates (Cahill, 2006). Some approaches to prevent postprandial hyperglycemia have thus far been reduction of dietary carbohydrate content, a change in the type of dietary carbohydrates, and ingestion of dietary fiber with meals (Schulze et al., 2004). However, the ideal type of pattern of ingestion of carbohydrate that minimize postprandial hyperglycemia is unknown.

Insulin, secreted from the pancreatic β cells, performs a pivotal role in homeostatic regulation of blood glucose levels. Insulin acts on the target organs such as muscle and liver, to promote uptake of glucose from the blood and suppress hepatic glucose production. Consequently, insulin decreases blood glucose levels and promotes the rapid recovery of increase in

71 postprandial blood glucose. As blood glucose levels decrease, insulin secretion also decreases.
72 Thus, the blood glucose level is maintained within a narrow normal range by the feedback
73 relationship between blood glucose and insulin (Castillo et al., 1994).

74 Although insulin secretion is regulated mainly by blood glucose, it is also regulated by a
75 family of circulating hormones called incretins (Seino et al., 2010). Incretins are hormones
76 secreted from the gastrointestinal tract upon food ingestion, these hormones act on pancreatic β
77 cells to promote insulin secretion. Gastric inhibitory polypeptide (GIP) and glucagon-like
78 peptide-1 (GLP-1) are incretins (Fujimoto et al., 2009; Preitner et al., 2004; Seino et al., 2010;
79 Vollmer et al., 2008). GIP is secreted from K cells of the upper small intestine (Inagaki et al.,
80 1989; Takeda et al., 1987); GLP-1 is secreted from L cells of the lower small intestine (Bell et
81 al., 1983; Orskov et al., 1993). Orally ingested glucose promotes incretin secretion into the
82 small intestine, where it is absorbed and enters the blood. Blood glucose and incretin act
83 cooperatively on pancreatic β cells to promote insulin secretion and increase circulating insulin
84 levels (Parkes et al., 2001).

85 Postprandial hyperglycemia is identified with an oral glucose tolerance test (OGTT), in which
86 a subject's ability to tolerate a glucose load (glucose tolerance) is evaluated by measuring blood

87 glucose level after an overnight fast and again 2 h after a 75-g oral glucose load (Stumvoll et al.,
88 2000). Using time course data of glucose and insulin in the blood during the OGTT, many
89 mathematical models have quantitatively evaluated the relationship between the blood glucose
90 and insulin in humans (Bergman et al., 1979; Brubaker et al., 2007; Dalla Man et al., 2016,
91 2013, 2007, 2006; De Gaetano et al., 2013; Hill et al., 1997; Kabul et al., 2015; Kim et al.,
92 2014; Overgaard et al., 2006; Pedersen et al., 2011; Riz et al., 2014; Røge et al., 2017; Salinari
93 et al., 2011; Tura et al., 2001). These models consist of blood glucose and insulin, but not
94 incretins (Bergman et al., 1979; Dalla Man et al., 2007, 2006; De Gaetano et al., 2013; Tura et
95 al., 2001). Other mathematical models incorporate the incretins (Brubaker et al., 2007; Dalla
96 Man et al., 2016; Kabul et al., 2015; Kim et al., 2014; Pedersen et al., 2011). In some models,
97 blood glucose and incretin act independently on insulin secretion during the OGTT (Brubaker et
98 al., 2007; Kabul et al., 2015; Kim et al., 2014); in others, blood glucose and incretin act
99 cooperatively (Dalla Man et al., 2016; Pedersen et al., 2011). The effective action of incretins on
100 the insulin secretion in mathematical models remains to be determined.

101 One application of mathematical models is the ability to make prediction. Published
102 mathematical models of blood glucose and insulin have been used to predict blood glucose

103 levels after glucose administration. We require a solution of a pair of forward and inverse
104 problems to obtain an optimal design of input pattern. Firstly, we need a dynamics model to
105 predict the temporal pattern as a consequence of a given input pattern. This mode of prediction
106 is a forward problem: The prediction is an “output pattern” related to the input pattern. Secondly,
107 optimal input pattern should be determined so as to minimize the outcome that is defined as an
108 arbitrarily given objective function of the predicted output pattern. This mode of prediction is an
109 inverse problem: The prediction is an “input pattern” that produces an optimal output pattern.
110 There are many established methods that use complex ordinary differential equations to solve
111 the forward problem of predicting output patterns, but few methods exist to solve the inverse
112 problem of predicting input patterns. Recently, we proposed a mathematical framework to
113 estimate an input pattern that produces a defined output pattern (Murakami et al., 2017).
114 Here, we constructed mathematical models with either glucose-independent and/or
115 glucose-cooperative roles of incretins on insulin secretion. We used the models to predict an
116 optimal glucose ingestion pattern that controls blood glucose level. Because blood glucose level
117 is the output pattern, this represents using the model to solve an inverse problem. We measured
118 blood glucose, insulin, GIP and GLP-1 before and after oral glucose ingestion with different

doses and ingestion durations for three subjects. As a forward problem, we constructed a mathematical model of blood glucose (output) in response to orally ingested glucose (input) for each subject. As an inverse problem, we optimally designed glucose ingestion pattern that minimized the peak value of blood glucose level for each subject. Each subject had an optimized pattern of ingestion that was intermittent. We validated blood glucose level by the predicted intermittent ingestion pattern for each subject and found that the intermittent ingestion pattern decreased the peak value of blood glucose level compared with the blood glucose levels that occurred with bolus or 1 h-continuous ingestion patterns. Thus, we provide the logical design of oral glucose ingestion pattern that minimizes the peak value of blood glucose level in humans, using an approach of combination of a forward and an inverse problems, which can be widely applied to design optimal dietary ingestion patterns for human health.

RESULTS

Measurement of Blood Glucose and Blood Hormones Before and After Oral Glucose Ingestion

To obtain the data for developing the model, we monitored the effect of ingestion of different amounts of glucose in different temporal patterns of ingestion on blood glucose and hormone

levels (Figure 1). In 6 separate experiments, the three healthy volunteers either rapidly consumed one of three doses of glucose (25 g, 50 g, 75 g) or consumed the glucose over 2 hours (see STAR Methods A.1, A.2). The rapid ingestion paradigm is referred to as bolus ingestion and the slow ingestion paradigm as 2 h-continuous ingestion. Prior to glucose ingestion and after glucose ingestion, we measured levels of blood glucose, insulin, C-peptide, intact GIP (designated GIP hereafter), and intact GLP-1 (designated GLP-1 hereafter) (see STAR Methods A.2).

With any ingestion pattern, the temporal pattern of each molecule exhibited a transient increase that returned to baseline within 4 hours (Figure 2). For bolus ingestion, the blood glucose and other blood hormones reached similar peak values for each dose of ingested glucose (Figure 2A, C, E, G, I). For the 2 h-continuous ingestion, blood glucose and other blood hormones showed increasing peak values with increasing doses of ingested glucose (Figure 2B, D, F, H, J). A consistent difference between bolus and continuous ingestion was that in the bolus ingestion case, with increasing doses of glucose, the time when blood glucose and hormones began to decrease and time to return to baseline become more delayed. In contrast, for 2 h-continuous ingestion, the time when blood glucose and other hormones began to decrease,

and the time when all returned to the basal level were similar regardless of dose of ingested glucose. Subjects #2 and #3 showed similar responses to subject #1 by bolus and 2 h-continuous ingestion, except for GLP-1 (Figure S1). GLP-1 for only 75 g bolus ingestion for subject #1 showed a high transient peak, but that for subjects #2 and #3 did not.

Mathematical Model of Blood Glucose Control

As a solution to the forward problem, we constructed a mathematical model of blood glucose control that fits time course data of blood glucose and hormones. We constructed a mathematical model from ordinary differential equations (Figure 3A, Table 1, Table S1, see STAR Methods B.1). Because of possible alternative mechanisms of actions of GIP and GLP-1 on insulin secretion (Brubaker et al., 2007; Dalla Man et al., 2016; Kabul et al., 2015; Kim et al., 2014; Pedersen et al., 2011), we constructed multiple alternative models in which the GIP or GLP-1 or both have independent actions or cooperative actions with blood glucose to promote insulin secretion (Figure 3A, Table 1, Table S1, see STAR Methods B.1). We estimated parameters of each model for each subject separately to fit time course data of blood glucose and hormones. We selected the best model of blood glucose control for each subject by Akaike Information Criterion (AIC) (see STAR Methods B.2). The selected models were the same for

167 subjects #1 and #3, but different from the model for subject #2 (Table S2, S3). In the models of
168 subject #1 and #3, cooperative action by blood glucose and GIP was selected, indicating that
169 insulin secretion did not depend on GLP-1. In the model of subject #2, the independent action of
170 GIP and Cooperative action by blood glucose and GLP-1 were selected. In each subject model,
171 time course data of each blood glucose and hormones were approximately reproduced (Figure
172 3B, Figure S2, S3, Table S4).

173 **Optimization and Validation of Glucose Ingestion Pattern that Minimizing Peak Value of**
174 **Blood Glucose Level**

175 Using mathematical, we tackled the inverse problem of predicting an optimal input pattern
176 that optimally controls the output pattern. Here, input and output patterns are, specifically, time
177 courses of oral glucose ingestion and blood glucose level, respectively. The optimality of the
178 output pattern is defined as an objective function that is a function of the output pattern,
179 typically the peak value of blood glucose level. First, we optimized the glucose ingestion pattern
180 for each subject that minimized the typical objective function. Hereafter, we designate the
181 optimized patterns minimizing objective function as the minimization pattern. We searched the
182 solution under the following restrictions; total 50 g of glucose should be ingested within 60 min,

183 glucose is ingested every 5 min, at least 1 g is ingested at 0 min and the remaining 49 g of
184 glucose is distributed between 0 and 60 min. Because the combination of glucose ingestion
185 patterns is enormous ($62!/(49!\,13!)$), we obtained an optimal ingestion pattern using an
186 evolutionary programing-based optimization algorithm (see SART Methods B.3) (Bäck and
187 Schwefel, 1993). The minimization patterns for the three subjects were designed with the
188 above-explained method and shown in Fig. 4A.

189 The optimized minimization pattern of the subject #1 appeared to be an intermittent pattern
190 with 30-min intervals with most glucose ingested at 0 min (17 g) and 60 min (23 g), and smaller
191 amounts ingested at 30 min (8 g) and 35 min (2 g) (Figure 4A, Table S5). This pattern was
192 different from bolus and 1 h-continuous ingestions. The predicted blood glucose achieved with
193 the minimization pattern showed a bimodal temporal pattern with peaks from ~25 min to 50 min
194 and at ~80 min (Figure 4B, red line).

195 The optimized minimization patterns of subjects #2 and #3 appeared to be intermittent
196 patterns similar to the pattern of the subject #1 (Figure 4A; Table S5). Compared with subject
197 #1, for subjects #2 and #3, the optimized pattern of ingestion had some notable differences:
198 Ingestion amount of glucose at 0 min was less, the number of time points at ~30-min the

199 intermittent period during which glucose was ingested was larger, and the ingestion amount of
200 glucose at 60 min was larger. The predicted blood glucose level achieved with the minimization
201 pattern for subjects #2 and #3 showed a similar bimodal pattern to that for subject #1 (Figure 4B,
202 red line).

203 We also compared the simulated blood glucose levels produced with the minimization pattern
204 with those simulated for bolus or 1 h-continuous ingestion of 50 g of glucose. The predicted
205 minimization pattern produced a lower peak value of blood glucose level than either simulations
206 of bolus or 1 h-continuous ingestion using the subject-specific models (Figure 4B).

207 We validated the predicted blood glucose levels produced with the minimization patterns for
208 each subject. Each subject ingested glucose according to their specific optimized minimization
209 pattern (Table S5), and blood glucose levels were measured. (Figure 4C, red line). The peak
210 value of blood glucose level produced by ingestion according to the minimization pattern in
211 each subject was less than those produced by bolus and 1 h-continuous ingestion (Figure 4C,
212 Table S6). All subjects exhibited bimodal temporal patterns of blood glucose level. These
213 experimental results are consistent with the predictions except that first peak in blood glucose
214 level at ~30 min was lower than the second peak at ~80 min for subjects #1 and #2 and the peak

in blood glucose was delayed from the prediction for subject #3.

To examine how the key parts of the ingestion pattern that resulted in the pattern that minimized the peak value of blood glucose level, we simplified the ingestion pattern into a coarse-grained ingestion pattern (Figure 5). We generated a minimization pattern with 5 parameters (Figure 5A, see STAR Methods B.4), and examined the effect of parameters on the peak value of blood glucose level.

We coarse-grained the minimization pattern into three periods; start time (0 min) of the first bolus ingestion, continuous-like intermediate period, and the end time of the ingestion (Figure 5A, upper panel). The coarse-grained pattern was characterized by 5 parameters; the dose of ingested glucose at 0 min u_0, the start time of the intermediate period t_s, the duration of intermediate period Δt, the dose of ingested of glucose at the end time u_T, and the end time of the ingestion T (Figure 5A, see STAR Methods B.4). We changed the parameters, and examined the effect of each parameter on the peak value of blood glucose level (Figure 5B).

To determine the parameter sets of the coarse-grained minimization pattern, we fixed $T = 60$ [min], the same duration as Figure 4A, and identified the parameter set that minimized the peak value of blood glucose level of subject #1 (Figure 5B, larger symbols). The parameter set

$u_0 = 17$ [g], $u_{60} = 24$ [g], $t_s = 30$ [min], $\Delta t = 0$ [min] produced a minimum (174.07 mg/dL) value for the peak value of blood glucose level, and this value is equivalent to that (173.95 mg/dL) achieved with the minimization pattern (Table 2). The coarse-grained minimization pattern was almost the same as that of the minimization pattern of subject #1 obtained in Figure 4. This result indicates that the coarse-grained minimization pattern captures essential characteristics of the minimization pattern, such as the peak value of blood glucose level and the temporal pattern.

We examined the dependency of the parameters on the end time of ingestion T for minimizing the peak value of blood glucose level (Figure 5B, top). When $T \leq 40$ [min], $u_0 + u_T = 50$ [g], and, as T increases u_0 increases (Figure 5B, red line), and u_T decreases (Figure 5B, green line). Thus, when the total ingestion time is within 40 min, (i) there is no intermediate period, and (ii) as the total ingestion time increases, the dose of ingested glucose at 0 min increases and the dose of ingested glucose at the end time decreases. When $T > 40$ [min], both u_0 and u_T decrease as T increases, and the dose of ingested glucose at the intermediate period $50 - u_0 - u_T$ increases almost linearly (Figure 5B, blue line). Thus, as the total ingestion time is longer than 40 minutes, (i) the dose of ingested glucose both at 0 min and

at the end time decrease and (ii) the dose ingested during the intermediate period increases. Also, when $T > 40$ [min], t_s is almost constant between 20 [g] and 30 [g] (Figure 5B, magenta line). Δt is nearly 0 [min] when $T \leq 60$ [min], and increases almost linearly when $T > 60$ [min] (Figure 5B, cyan line). Together these simulations indicated that, when the total ingestion time is shorter than 60 min, the duration of the intermediate period becomes so short that ingestion becomes bolus-like, and the intermediate period becomes longer as the total ingestion time is longer than 60 min. For subjects #2 and #3, the dependency of the parameters on the end time of ingestion T was also qualitatively the same (Figure 5B, middle and bottom).

Changing the duration of intermediate period Δt caused the greatest differences among the subjects (Figure S4). When $T = 60$ [min], the duration of the intermediate period of subject # 1 is shorter than those of subject #2 and #3, which was also shown in non-coarse-grained minimization patterns for the subjects (see Figure 4). For both subjects #2 and #3, as the total ingestion time becomes shorter than 60 min, the duration of the intermediate period becomes shorter and ingestion becomes bolus-like as for subject #1 (Figure 5B, Figure S4). Thus, the length of the total ingestion time is predicted to control the duration of the intermediate period among the subjects with all subjects exhibiting a point at which a bolus-like ingestion occurs

during the intermediate period.

The quantitative difference of duration of intermediate period among subjects may relate to differences in glucose tolerance among subjects. Glucose tolerance is determined by the balance between insulin secretion, sensitivity, and clearance; as glucose tolerance decreases, insulin secretion, sensitivity, and clearance also decrease (Antuna-Puente et al., 2011; Ohashi et al., 2018, 2015; Polidori et al., 2016; Schofield and Sutherland, 2012). Therefore, we examined the effect of the parameters for the reaction rates for insulin secretion, sensitivity and clearance on duration of the intermediate period (Figure S5). The models for each subject showed that the duration of the intermediate period becomes longer as the insulin secretion or sensitivity increase and becomes shorter as the insulin clearance increases. Thus, the duration of the intermittent period does not correspond to these insulin-related parameters controlling glucose tolerance.

DISCUSSION

Prediction and Validation of Glucose Ingestion Patterns that Minimize the Peak Value of Blood Glucose Level

In this study, as a forward problem, we constructed a mathematical model of the change in

279 blood glucose from time course data of blood glucose and hormones in blood during and
280 following oral glucose ingestion with various doses and durations in human subjects. Using this
281 model, as an inverse problem, we optimized glucose ingestion patterns that minimize the peak
282 value of blood glucose level and validated these patterns with the human subjects by
283 experiments. The minimization pattern was an intermittent pattern different from both the bolus
284 ingestion and the continuous ingestion. This intermittent ingestion pattern was intuitively not
285 obvious. However, we discovered the pattern using this approach of both constructing a
286 mathematical model as a forward problem and optimizing input pattern from the model as an
287 inverse problem. Although the best fitting model for each subject had important differences in
288 the roles of the blood hormones, the intermittent pattern as an optimal ingestion pattern to
289 minimize peak value of blood glucose level was common to all three subjects, suggesting that
290 the minimization pattern is robust to these differences in the model. Although we determined
291 that the duration of the intermittent period was a key parameter controlling the minimization
292 pattern output, we did not determine a molecular mechanism for how the intermittent pattern
293 minimizes the peak value of blood glucose level. This question will be analyzed in the future.
294 Methodologically, construction of a mathematical model based on the experimental data as a

295 forward problem is well-known. However, the inverse problem of optimizing an input pattern
296 to achieve a specified output pattern is challenging (Murakami et al., 2017). Our success in
297 identifying optimal input patterns through analysis of both the forward problem and inverse
298 problem suggests that this approach is valid for biological systems. An obvious potential
299 application is designing optimal ingestion patterns for various nutrients or combinations of
300 nutrients such that the ingestion pattern that minimizes the peak value of blood glucose level
301 can be logically designed. Such logical design of optimal food ingestion pattern will contribute
302 the human metabolic care and the prevention of the type 2 diabetes. Here, the objective
303 function for which we predict the input pattern is the peak value of the blood glucose level. By
304 changing the objective function, this approach can evaluate other biological outputs and
305 predict the input pattern that optimizes molecular concentrations or other measurable factors.

306 **Identification of Individualized Models of the Control of Blood Glucose Level**

307 Our ordinary differential equation models include the roles of incretins in insulin secretion.
308 By determining the best fitting model for each subject, we observed differences between
309 subjects in the roles of incretins in regulating blood glucose level. None of the subjects had
310 models that included an independent effect of GLP-1 on insulin secretion. Two of the three

311 subjects had no role for GLP-1 (independent or cooperative with glucose) in their optimal
312 models. In previous mathematical models using Caucasians data, only GLP-1, but not GIP, were
313 incorporated (Dalla Man et al., 2016; Pedersen et al., 2011). It has been reported that secretion
314 of intact GLP-1 in Japanese is very small, although that of the total GLP-1 in Japanese is almost
315 the same as that in Caucasians (Seino et al., 2010). All subjects in this study are Japanese, and,
316 the intact GIP level was higher than the intact GLP-1 level for all of them (Figure 2). Intact
317 GLP-1 and intact GIP have a similar EC_{50} for their receptors: The EC_{50} of intact GIP is 8 nM
318 (Gespach et al., 1984), and the EC_{50} of intact GLP-1 is 2.6 nM (Adelhorst et al., 1994).
319 Considering the higher level of intact GIP than intact GLP-1 in the blood and their similar
320 sensitivities, it is reasonable that intact GIP rather than intact GLP-1 was the incretin with the
321 most effect on insulin secretion in the best fitting model.

322 Many mathematical models use average values of blood glucose from many subjects of all
323 subjects. Some models that use data from individual subjects used data with only a single dose
324 of glucose (Dalla Man et al., 2013; De Gaetano et al., 2013; Ohashi et al., 2018, 2015). Here,
325 we used data from individual subjects using 3 different doses and 2 different durations of
326 glucose ingestion. We constructed a mathematical model using a single dose of glucose (75 g,

like that of the OGTT) in subject #1 and compared this OGTT model with the model that we constructed from the data for the 3 different doses and 2 different durations of glucose ingestion (Figure S6). The model that used the multiple dose and ingestion durations had a better fit to the blood glucose level achieved by ingestion of glucose according to the minimization pattern (lower RSS value) than did the model using 75 g OGTT alone. Thus, the single dose OGTT appears insufficient to reflect the dynamics of the blood glucose level in sufficient detail for mathematical modeling, and models should be constructed from data on multiple doses and durations of glucose ingestion to be useful in predicting the minimization pattern.

This finding that more training data provides more accurate predictive power is expected. However, the number of conditions for training data sets is limited in humans, because these types of studies take a long period of time and require several hours and fasting by the participants for each experimental condition. Here, we set an interval of 1 to 2 months for each experiment, thus collecting the data required a minimum of six months, and, in reality, more than a year. During such a long period, having many subjects for blood sampling following oral glucose ingestion every month over a year is difficult. Changes in the state of a subject can change during the months of the experiment, which can affect the model and reduce predictive

343 power. Thus, in human subject tests, there is a trade-off relationship between the number of
344 training data sets and the prediction accuracy.

345 A limitation of the study is that the model is limited. There are mechanisms, such as glucagon,
346 autonomic nerves, and free fatty acids, that did not incorporate into the model. Glucagon is a
347 counter-acting hormone to insulin in regulation of blood glucose. Glucagon increases blood
348 glucose level by facilitating glycogenolysis (Alberti and Zimmet, 1998; Jiang and Zhang, 2003).
349 Autonomic nerves not only regulates secretion of insulin and glucagon (Thorens, 2011), but also
350 affects hepatic glucose production and uptake (Kimura et al., 2016; Ruud et al., 2017). Free
351 fatty acids weakens the effect of insulin on hepatic glucose production and peripheral glucose
352 uptake (Okuno et al., 1998; Yamauchi et al., 2001). Although glucagon and free fatty acid are
353 not explicitly incorporated in our model, blood glucose levels and other hormone concentrations
354 are well reproduced, which may suggest that the effects of other molecules such as glucagon
355 and free fatty acid, are implicitly incorporated by some parameters in the model. Incorporating
356 glucagon and free fatty acid explicitly into the model is a future goal.

357 In conclusion, the key points of this study are three. The first point is the experimental design.
358 We performed six different conditions of oral glucose ingestion (3 doses and 2 durations) for

each subject and obtained detailed time course data, which makes the model predictable. The second point is the demonstration of ability to logically design blood glucose control. We predicted and validated the oral glucose ingestion pattern that minimized the peak value of blood glucose level. The third point is the methodology. We solved a forward problem by constructing the mathematical model of output with the given input patterns, and in turn, solved an inverse problem by logical designing the input pattern to control the output pattern. We expect that this approach with a forward problem and an inverse problem that are solved using the mathematical model can be widely applied to design optimal dietary ingestion pattern relevant to human health.

STAR★Methods

Detailed methods are provided in the online version of this paper and include the following:

- ●METHOD DETAILS
  - ○A. Experiment
  - ○B. Model and Analysis

SUPPLEMENTAL INFORMATION

Supplemental Information includes eight figures and seven tables.

AUTHOR CONTRIBUTIONS

Conceptualization and Methodology, M.F., Y.M., S.O. and S.K.;

Experiment, Y.K., Y.S., and S.F.;

Modeling and Simulation, M.F., and Y.M.;

Analysis, M.F., Y.M., M.K., S.U., H.K., H.I., K.K., S.O., S.I, S.K.;

Writing, M.F., Y.M., Y.K., and S.K.;

Supervision and Funding, S.I. and S.K.

ACKNOWLEDGEMENT

We thank fellow laboratory members for critical reading of the manuscript and for technical

385 assistance with the experiment and analysis. We thank Rika Sumita, Mina Shiguma, and Naomi
386 Isene for technical assistance. We thank Nancy R. Gough (BioSerendipity, LLC) for editing the
387 manuscript. The computations for this work were performed in part on the NIG supercomputer
388 system at ROIS National Institute of Genetics. This work was supported by the Creation of
389 Fundamental Technologies for Understanding and Control of Biosystem Dynamics
390 (JPMJCR12W3), CREST, of the Japan Science and Technology Agency (JST) and by the Japan
391 Society for the Promotion of Science (JSPS) KAKENHI Grant Number (17H06300, 17H6299,
392 18H03979). M.F. receives funding from a Grant-in-Aid for Challenging Exploratory Research
393 (16K12508). Y.K. receives funding from a Grant-in-Aid for Young Scientists (18K16578). S.U.
394 receives funding from a Grant-in-Aid for Scientific Research on Innovative Areas (16H01551)
395 and a Grant-in-Aid for Scientific Research on Innovative Areas (18H04801). H.K. receives
396 funding from a Grant-in-Aid for Scientific Research on Innovative Areas (16H06577). K.K.
397 receives funding from a Grant-in-Aid for Scientific Research (B) (15KT0021) and (C)
398 (15K00246), and a Grant-in-Aid for Scientific Research on Innovative Areas (16H01554). The
399 funders had no role in study design, data collection and analysis, decision to publish, or
400 preparation of the manuscript.

401

402 **REFERENCES**

403 Abdul-Ghani, M. a., Tripathy, D., DeFronzo, R.A., 2006. Contributions of beta-cell dysfunction
404 and insulin resistance to the pathogenesis of impaired glucose tolerance and impaired
405 fasting glucose. Diabetes Care 29, 1130–9. doi:10.2337/diacare.2951130
406 Adelhorst, K., Hedegaard, B.B., Knudsen, L.B., Kirk, O., 1994. Structure-activity studies of
407 glucagon-like peptide-1. J. Biol. Chem. 269, 6275–8.
408 Alberti, K.G., Zimmet, P.Z., 1998. Definition, diagnosis and classification of diabetes mellitus
409 and its complications. Part 1: diagnosis and classification of diabetes mellitus provisional
410 report of a WHO consultation. Diabet. Med. 15, 539–53.
411 doi:10.1002/(SICI)1096-9136(199807)15:7<539::AID-DIA668>3.0.CO;2-S
412 Antuna-Puente, B., Disse, E., Rabasa-Lhoret, R., Laville, M., Capeau, J., Bastard, J.-P., 2011.
413 How can we measure insulin sensitivity/resistance? Diabetes Metab. 37, 179–88.
414 doi:10.1016/j.diabet.2011.01.002
415 Bäck, T., Schwefel, H.-P., 1993. An Overview of Evolutionary Algorithms for Parameter
416 Optimization. Evol. Comput. 1, 1–23. doi:10.1162/evco.1993.1.1.1
417 Bell, G.I., Santerre, R.F., Mullenbach, G.T., 1983. Hamster preproglucagon contains the
418 sequence of glucagon and two related peptides. Nature 302, 716–8. doi:10.1038/302716a0
419 Bergman, R.N., Ider, Y.Z., Bowden, C.R., Cobelli, C., 1979. Quantitative estimation of insulin
420 sensitivity. Am. J. Physiol. 236, E667-77. doi:10.1172/JCI112886
421 Brubaker, P.L., Ohayon, E.L., D'Alessandro, L.M., Norwich, K.H., 2007. A mathematical
422 model of the oral glucose tolerance test illustrating the effects of the incretins. Ann.
423 Biomed. Eng. 35, 1286–1300. doi:10.1007/s10439-007-9274-1
424 Cahill, G.F., 2006. Fuel metabolism in starvation. Annu. Rev. Nutr. 26, 1–22.
425 doi:10.1146/annurev.nutr.26.061505.111258
426 Castillo, M.J., Scheen, A.J., Letiexhe, M.R., Lefèbvre, P.J., 1994. How to measure insulin
427 clearance. Diabetes. Metab. Rev. 10, 119–50.
428 Dalla Man, C., Camilleri, M., Cobelli, C., 2006. A system model of oral glucose absorption:
429 validation on gold standard data. IEEE Trans. Biomed. Eng. 53, 2472–8.
430 doi:10.1109/TBME.2006.883792

Dalla Man, C., Micheletto, F., Sathananthan, M., Vella, A., Cobelli, C., 2016. Model-Based Quantification of Glucagon-Like Peptide-1-Induced Potentiation of Insulin Secretion in Response to a Mixed Meal Challenge. Diabetes Technol. Ther. 18, 39–46. doi:10.1089/dia.2015.0146

Dalla Man, C., Piccinini, F., Basu, R., Basu, A., Rizza, R. a, Cobelli, C., 2013. Modeling hepatic insulin sensitivity during a meal: validation against the euglycemic hyperinsulinemic clamp. Am. J. Physiol. Endocrinol. Metab. 304, E819-25. doi:10.1152/ajpendo.00482.2012

Dalla Man, C., Raimondo, D.M., Rizza, R. a., Cobelli, C., 2007. GIM, Simulation Software of Meal Glucose--Insulin Model. J. Diabetes Sci. Technol. 1, 323–330. doi:10.1177/193229680700100303

De Gaetano, A., Panunzi, S., Matone, A., Samson, A., Vrbikova, J., Bendlova, B., Pacini, G., 2013. Routine OGTT: a robust model including incretin effect for precise identification of insulin sensitivity and secretion in a single individual. PLoS One 8, e70875. doi:10.1371/journal.pone.0070875

Edelstein, S.L., Knowler, W.C., Bain, R.P., Andres, R., Barrett-Connor, E.L., Dowse, G.K., Haffner, S.M., Pettitt, D.J., Sorkin, J.D., Muller, D.C., Collins, V.R., Hamman, R.F., 1997. Predictors of progression from impaired glucose tolerance to NIDDM: an analysis of six prospective studies. Diabetes 46, 701–10.

Fujimoto, W., Miki, T., Ogura, T., Zhang, M., Seino, Y., Satin, L.S., Nakaya, H., Seino, S., 2009. Niflumic acid-sensitive ion channels play an important role in the induction of glucose-stimulated insulin secretion by cyclic AMP in mice. Diabetologia 52, 863–872. doi:10.1007/s00125-009-1306-y

Gespach, C., Emami, S., Rosselin, G., 1984. Gastric inhibitory peptide (GIP), pancreatic glucagon and vasoactive intestinal peptide (VIP) are cAMP-inducing hormones in the human gastric cancer cell line HGT-1. Homologous desensitization of VIP receptor activity. Biochem. Biophys. Res. Commun. 120, 641–9.

Hill, K., Caprihan, A., Kakalios, J., 1997. Bulk Segregation in Rotated Granular Material Measured by Magnetic Resonance Imaging. Phys. Rev. Lett. 78, 50–53. doi:10.1103/PhysRevLett.78.50

Inagaki, N., Seino, Y., Takeda, J., Yano, H., Yamada, Y., Bell, G.I., Eddy, R.L., Fukushima, Y., Byers, M.G., Shows, T.B., 1989. Gastric inhibitory polypeptide: structure and

463 chromosomal localization of the human gene. Mol. Endocrinol. 3, 1014–21.
464 doi:10.1210/mend-3-6-1014
465 Jiang, G., Zhang, B.B., 2003. Glucagon and regulation of glucose metabolism. Am. J. Physiol.
466 Endocrinol. Metab. 284, E671-8. doi:10.1152/ajpendo.00492.2002
467 Kabul, R.S.E., Kabul, E., Pratiwi, A., Setiawan, A.A., Dahlan, K., Kartono, A., 2015.
468 Mathematical Model of Glucose-Insulin System Using the Modified Oral Minimal Model
469 and the Incretin Effects. Int. J. Pharm. Pharm. Sci. 7, 451–454.
470 Kim, M., Oh, T.J., Lee, J.C., Choi, K., Kim, M.Y., Kim, H.C., Cho, Y.M., Kim, S., 2014.
471 Simulation of oral glucose tolerance tests and the corresponding isoglycemic intravenous
472 glucose infusion studies for calculation of the incretin effect. J. Korean Med. Sci. 29,
473 378–85. doi:10.3346/jkms.2014.29.3.378
474 Kimura, K., Tanida, M., Nagata, N., Inaba, Y., Watanabe, H., Nagashimada, M., Ota, T.,
475 Asahara, S., Kido, Y., Matsumoto, M., Toshinai, K., Nakazato, M., Shibamoto, T., Kaneko,
476 S., Kasuga, M., Inoue, H., 2016. Central Insulin Action Activates Kupffer Cells by
477 Suppressing Hepatic Vagal Activation via the Nicotinic Alpha 7 Acetylcholine Receptor.
478 Cell Rep. 14, 2362–74. doi:10.1016/j.celrep.2016.02.032
479 Miyawaki, K., Yamada, Y., Ban, N., Ihara, Y., Tsukiyama, K., Zhou, H., Fujimoto, S., Oku, A.,
480 Tsuda, K., Toyokuni, S., Hiai, H., Mizunoya, W., Fushiki, T., Holst, J.J., Makino, M.,
481 Tashita, A., Kobara, Y., Tsubamoto, Y., Jinnouchi, T., Jomori, T., Seino, Y., 2002.
482 Inhibition of gastric inhibitory polypeptide signaling prevents obesity. Nat. Med. 8,
483 738–42. doi:10.1038/nm727
484 Murakami, Y., Koyama, M., Oba, S., Kuroda, S., Ishii, S., 2017. Model-based control of the
485 temporal patterns of intracellular signalingin silico. Biophys. physicobiology 14, 29–40.
486 doi:10.2142/biophysico.14.0_29
487 Nakagami, T., DECODA Study Group, 2004. Hyperglycaemia and mortality from all causes
488 and from cardiovascular disease in five populations of Asian origin. Diabetologia 47,
489 385–394. doi:10.1007/s00125-004-1334-6
490 Ohashi, K., Fujii, M., Uda, S., Kubota, H., Komada, H., Sakaguchi, K., Ogawa, W., Kuroda, S.,
491 2018. Increase in hepatic and decrease in peripheral insulin clearance characterize
492 abnormal temporal patterns of serum insulin in diabetic subjects. npj Syst. Biol. Appl. 4,
493 14. doi:10.1038/s41540-018-0051-6
494 Ohashi, K., Komada, H., Uda, S., Kubota, H., Iwaki, T., Fukuzawa, H., Komori, Y., Fujii, M.,

Toyoshima, Y., Sakaguchi, K., Ogawa, W., Kuroda, S., 2015. Glucose Homeostatic Law: Insulin Clearance Predicts the Progression of Glucose Intolerance in Humans. PLoS One 10, e0143880. doi:10.1371/journal.pone.0143880

Okuno, A., Tamemoto, H., Tobe, K., Ueki, K., Mori, Y., Iwamoto, K., Umesono, K., Akanuma, Y., Fujiwara, T., Horikoshi, H., Yazaki, Y., Kadowaki, T., 1998. Troglitazone increases the number of small adipocytes without the change of white adipose tissue mass in obese Zucker rats. J. Clin. Invest. 101, 1354–61. doi:10.1172/JCI1235

Orskov, C., Wettergren, A., Holst, J.J., 1993. Biological effects and metabolic rates of glucagonlike peptide-1 7-36 amide and glucagonlike peptide-1 7-37 in healthy subjects are indistinguishable. Diabetes 42, 658–61.

Overgaard, R. V, Jelic, K., Karlsson, M., Henriksen, J.E., Madsen, H., 2006. Mathematical beta cell model for insulin secretion following IVGTT and OGTT. Ann. Biomed. Eng. 34, 1343–54. doi:10.1007/s10439-006-9154-0

Parkes, D.G., Pittner, R., Jodka, C., Smith, P., Young, A., 2001. Insulinotropic actions of exendin-4 and glucagon-like peptide-1 in vivo and in vitro. Metabolism. 50, 583–589. doi:10.1053/meta.2001.22519

Pedersen, M.G., Dalla Man, C., Cobelli, C., 2011. Multiscale modeling of insulin secretion. IEEE Trans. Biomed. Eng. 58, 3020–3. doi:10.1109/TBME.2011.2164918

Polidori, D.C., Bergman, R.N., Chung, S.T., Sumner, A.E., 2016. Hepatic and Extrahepatic Insulin Clearance Are Differentially Regulated: Results From a Novel Model-Based Analysis of Intravenous Glucose Tolerance Data. Diabetes 65, 1556–64. doi:10.2337/db15-1373

Preitner, F., Ibberson, M., Franklin, I., Binnert, C., Pende, M., Gjinovci, A., Hansotia, T., Drucker, D.J., Wollheim, C., Burcelin, R., Thorens, B., 2004. Gluco-incretins control insulin secretion at multiple levels as revealed in mice lacking GLP-1 and GIP receptors. J. Clin. Invest. 113, 635–645. doi:10.1172/JCI200420518

Riz, M., Pedersen, M.G., Toffolo, G.M., Haschke, G., Schneider, H.-C., Klabunde, T., Margerie, D., Cobelli, C., 2014. Minimal modeling of insulin secretion in the perfused rat pancreas: a drug effect case study. Am. J. Physiol. Endocrinol. Metab. doi:10.1152/ajpendo.00603.2013

Røge, R.M., Bagger, J.I., Alskär, O., Kristensen, N.R., Klim, S., Holst, J.J., Ingwersen, S.H., Karlsson, M.O., Knop, F.K., Vilsbøll, T., Kjellsson, M.C., 2017. Mathematical Modelling

of Glucose-Dependent Insulinotropic Polypeptide and Glucagon-like Peptide-1 following Ingestion of Glucose. Basic Clin. Pharmacol. Toxicol. 38, 42–49. doi:10.1111/bcpt.12792

Ruud, J., Steculorum, S.M., Brüning, J.C., 2017. Neuronal control of peripheral insulin sensitivity and glucose metabolism. Nat. Commun. 8, 15259. doi:10.1038/ncomms15259

Salinari, S., Bertuzzi, A., Mingrone, G., 2011. Intestinal transit of a glucose bolus and incretin kinetics: a mathematical model with application to the oral glucose tolerance test. Am. J. Physiol. Endocrinol. Metab. 300, E955-65. doi:10.1152/ajpendo.00451.2010

Sano, T., Kawata, K., Ohno, S., Yugi, K., Kakuda, H., Kubota, H., Uda, S., Fujii, M., Kunida, K., Hoshino, D., Hatano, A., Ito, Y., Sato, M., Suzuki, Y., Kuroda, S., 2016. Selective control of up-regulated and down-regulated genes by temporal patterns and doses of insulin. Sci. Signal. 9, ra112. doi:10.1126/scisignal.aaf3739

Schofield, C.J., Sutherland, C., 2012. Disordered insulin secretion in the development of insulin resistance and Type 2 diabetes. Diabet. Med. 29, 972–9. doi:10.1111/j.1464-5491.2012.03655.x

Schulze, M.B., Liu, S., Rimm, E.B., Manson, J.E., Willett, W.C., Hu, F.B., 2004. Glycemic index, glycemic load, and dietary fiber intake and incidence of type 2 diabetes in younger and middle-aged women. Am. J. Clin. Nutr. 80, 348–356. doi:10.1093/ajcn/80.2.348

Seino, Y., Fukushima, M., Yabe, D., 2010. GIP and GLP-1, the two incretin hormones: Similarities and differences. J. Diabetes Investig. 1, 8–23. doi:10.1111/j.2040-1124.2010.00022.x

Stumvoll, M., Mitrakou, A., Pimenta, W., Jenssen, T., Yki-Jarvinen, H., Van Haeften, T., Renn, W., Gerich, J., 2000. Use of the oral glucose tolerance test to assess insulin release and insulin sensitivity. Diabetes Care 23, 295–301. doi:10.2337/diacare.23.3.295

Takeda, J., Seino, Y., Tanaka, K., Fukumoto, H., Kayano, T., Takahashi, H., Mitani, T., Kurono, M., Suzuki, T., Tobe, T., 1987. Sequence of an intestinal cDNA encoding human gastric inhibitory polypeptide precursor. Proc. Natl. Acad. Sci. U. S. A. 84, 7005–8. doi:10.1073/pnas.84.20.7005

Tholen, D.W., Kallner, A.J., Kennedy, W., Krouwer, J.S., Meier, K., 2004. Evaluation of Precision Performance of Quantitative Measurement Methods; Approved Guideline.

Thorens, B., 2011. Brain glucose sensing and neural regulation of insulin and glucagon secretion. Diabetes. Obes. Metab. 13 Suppl 1, 82–8. doi:10.1111/j.1463-1326.2011.01453.x

559 Tietz, N. (Ed.), 1990. Clinical Guide to Laboratory Tests, 2nd Edition. WB Saunders,
560 Philadelphia.
561 Tijssen, P., 1985. Practice and theory of enzyme immunoassays. Elsevier, Amsterdam, NY.
562 Tura, a, Ludvik, B., Nolan, J.J., Pacini, G., Thomaseth, K., 2001. Insulin and C-peptide
563 secretion and kinetics in humans: direct and model-based measurements during OGTT.
564 Am. J. Physiol. Endocrinol. Metab. 281, E966-74.
565 Vollmer, K., Holst, J.J., Baller, B., Ellrichmann, M., Nauck, M. a, Schmidt, W.E., Meier, J.J.,
566 2008. Predictors of incretin concentrations in subjects with normal, impaired, and diabetic
567 glucose tolerance. Diabetes 57, 678–87. doi:10.2337/db07-1124
568 Yamauchi, T., Kamon, J., Waki, H., Murakami, K., Motojima, K., Komeda, K., Ide, T., Kubota,
569 N., Terauchi, Y., Tobe, K., Miki, H., Tsuchida, A., Akanuma, Y., Nagai, R., Kimura, S.,
570 Kadowaki, T., 2001. The mechanisms by which both heterozygous peroxisome
571 proliferator-activated receptor gamma (PPARgamma) deficiency and PPARgamma
572 agonist improve insulin resistance. J. Biol. Chem. 276, 41245–54.
573 doi:10.1074/jbc.M103241200
574
575

STAR★Methods

KEY RESOURCE TABLE

REAGENT or RESOURCE	SOURCE	IDENTIFIER
Software and Algorithms		
Ordinary Differential Equation Simulations and Analysis - MATLAB	Mathworks	RRID:SCR_001622

METHOD DETAILS

A. Experiment

A.1. Subjects

The subjects' profiles are as shown in Table S7. All subjects are healthy, and signed informed consent.

A.2. Blood Sampling Experiment

For oral glucose tolerance test, a glucose solution containing 25 g, 50 g or 75 g glucose was orally ingested after a 10-hour fasting, and blood samples were obtained at the times indicated in the figures from the cutaneous vein of the forearm. Blood samples were obtained from the cutaneous vein of the forearm. Blood collection on fasting was performed twice and then a

588 glucose solution containing 25 g, 50 g or 75 g glucose was orally ingested. The ingestion
589 method was rapid within a minute (bolus ingestion), and continuous over the course of 2 hours
590 (2 h-continuous ingestion). For continuous ingestion, we connected the tube to noncontact
591 microdispenser robot (Mr. MJ; MECT Corporation) (Sano et al., 2016) and glucose solution was
592 ingested from tube. To equalize the volume of ingested glucose solution, glucose solution,
593 TRELAN-G75 (AJINOMOTO), was diluted with distilled water into a total volume 225 ml.
594 Each amount of glucose and delivery paradigm was tested with each subject in experiments
595 separated by at least 1 month. Blood was rapidly centrifuged, plasma glucose and hormone
596 concentrations expect for GIP were measured according to the methods with LSI Medience Co.,
597 Ltd. Plasma glucose was measured by enzymatic methods (IATRO LQ GLU). Plasma insulin
598 and Serum C-peptide was measured by Chemiluminescent Immunoassay (Tholen et al., 2004;
599 Tietz, 1990). Plasma intact GLP-1 and Plasma intact GIP were measured by ELISA kits
600 (#EGLP-35K, Merck, Billerica, MA or #27201, Immuno-Biological Laboratories, Gunma,
601 Japan, respectively) (Miyawaki et al., 2002; Tijssen, 1985). For simplicity, we refer to plasma
602 glucose, plasma insulin, serum C-peptide, plasma intact GIP, and plasma intact GLP-1 as blood
603 glucose, insulin, C-peptide, GIP, and GLP-1, respectively.

A.3. Validation Experiment

For the validation experiment of the minimization pattern, we employed the same method as described in A.2 for the subject #1, and a Freestyle Libre continuous glucose monitoring system (FGM; Abbott Diabetes Care) for subjects #2 and #3. FGM reduces the invasive burden on the subjects because the subjects wear a sensor rather than requiring an indwelling needle for blood glucose monitoring. We performed the experiment after the subject had worn the sensors for at least two days. Each subject wore three sensors, and bolus ingestion, continuous ingestion for 1 hour, ingestion of minimization pattern were carried out using the same sensors within two weeks. The results of the three sensors were averaged for each paradigm. Because FGM measures glucose level of the interstitial fluid rather than glucose level in the blood, the measured value reflects a delay of about 5 to 20 minutes (Figure S3) compared with the values obtained by blood collection.

A.4. Ethics Committee Certification

We complied with Japan's Ethical Guidelines for Epidemiological Research, and the study as approved by the ethics committees of the Life-Science Committee of the University of Tokyo (16-265). Subjects were recruited by the related law.

B. Model and Analysis

B.1. Model Structure and Parameter Structure

For each subject, we estimated parameters that reproduce the time course data of blood glucose, insulin, C-peptide, intact GIP, and intact GLP-1 of six glucose ingestion patterns, combinations of three doses (25 g, 50 g, and 75 g) and given by bolus and 2 h-continuous ingestion, using the following model (Equations 1–21, Table 1).

$$\frac{dIntest_G}{dt} = v_1 - v_6, \#(Equation\ 1)$$

$$\frac{dGIP}{dt} = v_2 + v_3, \#(Equation\ 2)$$

$$\frac{dGLP1}{dt} = v_4 + v_5, \#(Equation\ 3)$$

$$\frac{dRa_{GutG}}{dt} = v_6 - v_7, \#(Equation\ 4)$$

$$\frac{dG}{dt} = \frac{v_7}{V} + v_8 - v_9, \#(Equation\ 5)$$

$$\frac{dI}{dt} = v_{10} - v_{11}, \#(Equation\ 6)$$

$$\frac{dCP}{dt} = v_{10} - v_{12}, \#(Equation\ 7)$$

$$\frac{dX}{dt} = \frac{v_{11}}{k_{11}} - v_{13}, \#(Equation\ 8)$$

Equations 1-8 indicate differential equations reproducing time developments of glucose amount in the intestine $Intest_G$ [g], GIP level GIP [pM], GLP-1 level $GLP1$ [pM], rate of appearance

of ingested glucose amount into the blood Ra_{GutG} [g/min], blood glucose level G [mg/dL], insulin level I [pM], C-peptide CP [pM], and the insulin level acting on the regulation of glucose X (denoted as effective insulin concentration at target organs hereafter). Each variable is controlled by fluxes v_i $\{i = 1, \cdots, 13\}$. However, in Equation 5, v_7 was divided by the constant V to convert the ingested glucose amount into the blood glucose level. Also in Equation 8, v_{11} was divided by k_{11} to render X dimensionless. Rendering X dimensionless enables the elimination of redundant parameters, and improves the accuracy of parameter estimation. The fluxes v_i are given by

$$v_1 = Glucose, \#(Equation\ 9)$$

$$v_2 = \frac{k_2\ Intest_G}{K_2 + Intest_G}, \#(Equation\ 10)$$

$$v_3 = k_3\ (GIP_B - GIP), \#(Equation\ 11)$$

$$v_4 = \frac{k_4\ Intest_G}{K_4 + Intest_G}, \#(Equation\ 12)$$

$$v_5 = k_5\ (GLP1_B - GLP1), \#(Equation\ 13)$$

$$v_6 = \frac{k_6\ Intest_G}{K_6 + Intest_G}, \#(Equation\ 14)$$

$$v_7 = k_7\ Ra_{GutG}, \#(Equation\ 15)$$

$$v_8 = \frac{k_8}{K_8 + X}, \#(Equation\ 16)$$

$$v_9 = k_9\ G\ X, \#(Equation\ 17)$$

$$v_{10} = k_{10}(G + a\ GIP + b\ G\ GIP + c\ GLP1 + d\ G\ GLP1), \#(Equation\ 18)$$

$$v_{11} = \frac{k_{11}\ I}{K_{11} + I}, \#(Equation\ 19)$$

$$v_{12} = k_{12}\ CP, \#(Equation\ 20)$$

$$v_{13} = k_{13}\ X, \#(Equation\ 21)$$

(Table 1, Figure 3).

v_1 indicates the influx of ingested glucose into the intestine, given by dose of glucose ingestion divided by the time duration of ingestion Δt, otherwise 0 (Equation 22). For rapid ingestion, such as bolus ingestion, or for the ingestion of minimization pattern, Δt is assumed as 0.5 [min]. For example, in the case of 50 g bolus,

$$Glucose = \begin{cases} \text{dose}/\Delta t = 50/0.5 = 100, & 0 \le t < 0.5 \\ 0, & otherwise \end{cases}. \#(\text{Equation Error! Bookmark not defined.})$$

v_2 indicates the secretion of GIP depending on the glucose amount in the intestine ($Intest_G$).

v_3 indicates absorption of GIP by the intestine and entry into the blood, which is proportional to GIP subtracted by its basal GIP_B. At steady state without glucose ingestion, GIP converges to GIP_B. v_4 indicates the secretion of GLP-1 depending on the glucose amount in the intestine. v_5 indicates the absorption of GLP-1 proportional to $GLP1$ subtracted by its

basal $GLP1_B$. At the steady state without glucose ingestion, $GLP1$ converges to $GLP1_B$. v_6 indicates the flow of glucose from the intestine to the rate of appearance (Ra_{GutG}). With bolus ingestion, this flow can be regarded as constant because of the large amount of glucose in the intestine (Brubaker et al., 2007). Therefore, we assumed that this flux is given by the Michaelis-Menten equation, which saturates when the glucose amount is large. v_7 indicates the flow of glucose from the rate of appearance into the blood, which is proportional to the rate of appearance of ingested glucose amount. v_8 indicates the flow of glucose production from the liver into the blood, given by an inhibitory Michaelis-Menten equation, which decreases as the amount of effective insulin X increases. v_9 indicates the glucose uptake from the blood to the periphery and is given by the product between blood glucose level G and effective insulin X. v_{10} indicates the secretion of insulin. In this study, the actions of GIP and GLP-1 on insulin secretion were represented as independent actions of each incretin and as cooperative actions with blood glucose. By incorporating the parameters ($a, b, c,$ and d in Equation 18), we could relate insulin secretion to cooperative or independent actions using AIC (Akaike Information Criteria) to select the model that best fit the data (Table S1, S2). v_{11} indicates the flow of insulin I into target organs, such as liver and muscle, leading to effective insulin X. v_{12}

indicates inactivation of C-peptide CP and decreases in proportion to CP itself. v_{13} indicates the binding of X to the cells in the target organs in proportion to X itself.

For the model, parameters were estimated for each subject. Here, the estimated parameters are the 18 parameters of $k_2, k_3, k_4, k_5, k_6, k_7, k_8, k_{10}, K_2, K_4, K_6, K_8, K_{11}, V, a, b, c$ and d; and six initial levels of $GIP(0), GLP1(0), G(0), I(0), CP$ and $X(0)$. Using the variables, and assuming $Duod_G, Ra_{GutG}, GIP, GLP1, G, I, X,$ and CP are at steady state before ingestion, other initial conditions and parameters were determined by estimated parameters and initial values, given by

$$Ingest_G(0) = 0, \#(Equation\ 23)$$

$$Ra_{GutG}(0) = 0, \#(Equation\ 24)$$

$$k_9 = \frac{k_8}{G(0) \cdot X(0) \cdot (X(0) + K_8)}, \#(Equation\ 25)$$

$$k_{11} = k_{10} \frac{K_{11} + I(0)}{I(0)} \big(G(0) + a\ GIP(0) + b\ G(0)GIP(0) + c\ GLP1(0) + d\ G(0)GLP1(0)\big), \#(Equation\ 26)$$

$$k_{12} = \frac{k_{10}}{CP(0)} \big(G(0) + a\ GIP(0) + b\ G(0)GIP(0) + c\ GLP1(0) + d\ G(0)GLP1(0)\big), \#(Equation\ 27)$$

$$k_{13} = \frac{I(0)\ (I(0) + K_{11})}{X(0)}, \#(Equation\ 28)$$

$$GIP_B = GIP(0), \#(Equation\ 29)$$

$$GLP1_B = GLP1(0). \#(Equation\ 30)$$

These parameters are different between subjects, but the same for each subject for each experimental paradigm (dose and duration and ingestion). This means that the state for each subject does not change during this study. For time development, we used CVODE in Matlab's Systems biology toolbox.

We used the residual sum of squares as the objective function so that the residual between the experimental value and the simulation value is reduced, given by

$$RSS = \sum_i \sum_k \sum_t \left[\frac{x_{i,k}^{sim}(t) - x_{i,k}^{exp}(t)}{\max_t x_{i,k}^{exp}(t) - \min_t x_{i,k}^{exp}(t)} \right]^2 .\#(Equation\ 31)$$

$x_{i,k}^{sim}(t)$ and $x_{i,k}^{exp}(t)$ indicate the simulation values and the experimental values of molecular species $k \in \{G, I, CP, GLP1, GIP\}$ at time t in the experiment $i \in \{25B, 25C, 50B, 50C, 75B, 75C\}$, for which each experiment is denoted by the ingestion dose and the initial letters of the duration of ingestion, 25 g-bolus ingestion, 25B and for 75 g-2 h-continuous, 75C. To avoid the influences of the differences in the absolute quantities of the molecules, we normalized the difference between the simulation value and the experimental value by the difference between the maximum value and the minimum value of the experiment. We performed parameter estimation for global optimal solution using Evolutionary programming (Bäck and Schwefel, 1993) for 40 trials with a parent number of 5000 and a

generation number of 5000, then we obtained a local optimal solution using the simplex search method (Matlab fminsearch). We implemented all programs using Matlab 2015a and performed parameter estimation using 2.6 GHz CPU (Xeon E5 2670) at the National Institute of Genetics (NIG), Supercomputer System of Research Organization of Information and System (ROIS).

B.2. Model Selection

Using parameters of a, b, c and d in Equation 18, which indicate contributions to insulin secretion of incretins as independent actions of each incretin and cooperative actions with glucose, we considered the multiple models shown in Table S1.

We performed the parameter estimation of each of the above models using RSS of Equation 31 for each subject. Here, we assumed that each residual of the simulation value and the experiment value in Equation 31 follows a normal distribution. Among the models to be compared, the sum N of the numbers of data of each variable measured in the experiment is the same. Therefore, AIC (Akaike Information Criteria), which is a criterion of model selection can be calculated for each model, given by

$$AIC = N\,log(RSS) + 2K.\#(Equation\ 32)$$

We employed a model that minimizes AIC for each subject as a model representing the

700 dynamics of blood molecules in the subject. For the models not including GLP-1 of subjects #1
701 and #3 as mentioned below, we also calculated AIC for each model similar to those including
702 GLP-1.

703 The selected models for each subject were distinct (Table 2, Table S1, S2). For subject #1,
704 the best model had no influence of GLP-1 and both an independent action and cooperative
705 action with glucose for GIP (Table S2, $c = d = 0$), indicating that the insulin secretion of
706 subject #1 is independent of GLP-1. For subject #2, the best model had an independent action
707 of GIP and a cooperative action of GLP-1 with glucose (Table S2, $b = c = 0$), indicating that
708 the insulin secretion of subject #2 depends on both GIP and GLP-1. For subject #3, the best
709 model had only the cooperative action of GIP with glucose (Table S2, $a = c = d = 0$),
710 indicating that the insulin secretion of subject #3 is independent of GLP-1. In each subject
711 model, time course data of each blood glucose and hormones were approximately reproduced
712 (Figure 3B, Figure S2, S3).

713 In the selected models of subjects #1 and #3, insulin secretion did not depend on GLP-1,
714 therefore, we performed parameter estimation and model selection using models that did not
715 include GLP-1 by removing Equation 3. Insulin secretion using the best fitting of these models

for both subjects #1 and #3 included the term of independent action of blood glucose and the cooperative term of blood glucose and GIP (Table S3, $a = 0$). We used these models for subjects #1 and #3.

B.3. Estimation of Minimization Patterns

We set the oral glucose $u(t)$ as a function of time t [min] according to the following constraint condition. First, glucose was orally ingested at intervals of 5 min from 0 min to 60 min. Here, we defined u_s [g] as the dose of ingestion at the minute s [min] $(s = 0, 5, \ldots, 60)$ and $u_{0:60}$ as the temporal pattern of oral glucose ingestion, given by

$$\boldsymbol{u}_{0:60} = [u_0, u_5, \ldots, u_{60}]. \#(Equation\ 33)$$

Also, we set the total dose of glucose ingestion at 50 g, *i.e.* $\sum_s u_s = 50$ [g], each dose at s is the integer value with unit of 1 g, *i.e.* $u_s \in \mathbb{Z}, u_s \geq 0$, and at least 1 g is ingested at 0 min to start the ingestion, *i.e.* $u_0 \geq 1$. We assumed that ingestion at each time is taken over 0.5 min, and convert $u_{0:60}$ to $Glucose$ instead of Equation 9, given by

$$Glucose(t) = \begin{cases} u_s/0.5 & t_i \leq t < t_i + 0.5, \\ 0 & otherwise \end{cases} \qquad t_i \in \{0, 5, \cdots, 60\}. \#(Equation\ 34)$$

Next, we expressed a nonlinear ordinary differential equation model (Equations 1–8)

describing the dynamics of the glucose metabolism system, given by

$$\frac{d\boldsymbol{x}}{dt} = \boldsymbol{f}(u(t), \boldsymbol{x}(t); \boldsymbol{\theta}), \#(Equation\ 35)$$

$$\boldsymbol{x}(0) = \boldsymbol{x}^{init}, \#(Equation\ 36)$$

where $\boldsymbol{x}$ indicates a state variable, $\boldsymbol{x}^{init}$ indicates an initial state, $\boldsymbol{\theta}$ is a parameter set, and $\boldsymbol{f}$ is a nonlinear function. These types and values of $\boldsymbol{x}$, $\boldsymbol{x}^{init}$, $\boldsymbol{\theta}$, and $\boldsymbol{f}$ are different among subjects, because the selected models of subjects and parameters are different among subjects (see STAR Methods B.2). Each subject has one set of $\boldsymbol{f}$, $\boldsymbol{x}^{init}$, and θ. $\boldsymbol{x}(0{:}\,T)$. The temporal pattern of $\boldsymbol{x}$ from $t = 0$ to $t = T$ with the temporal pattern of oral glucose ingestion $\boldsymbol{u}_{0:60}$ can be obtained by the deterministic numerical simulation of this mathematical model Sim, given by

$$\boldsymbol{x}(0{:}\,T) = Sim\left(\boldsymbol{u}_{0:60}, \boldsymbol{x}^{init}, \boldsymbol{\theta}, \boldsymbol{f}, T\right). \#(Equation\ 37)$$

To design a temporal pattern of oral glucose ingestion that minimizes the peak value of blood glucose level, we formulated as an optimization problem. Defining the peak value of blood glucose level in the time course $x(0{:}\,T)$ as $G_{Max}\left(\boldsymbol{x}(0{:}\,T)\right)$ and setting the objective function of the optimization problem to be $J\left(G_{Max}\left(x(0{:}\,T)\right)\right)$, we set the objective functions for

743 designing the temporal patterns of oral glucose ingestion that minimizes the peak value of blood

744 glucose level, given by

$$J\left(G_{Max}\left(\boldsymbol{x}(0:T)\right)\right) = G_{Max}\left(\boldsymbol{x}(0:T)\right). \#(Equation\ 38)$$

745 Under these settings, the optimization problem of designing the oral glucose ingestion pattern

746 can be expressed as follows for minimizing the peak value of blood glucose level, given by

$$\underset{\boldsymbol{u}_{0:60}}{argmin}\, J\left(G_{Max}\left(\boldsymbol{x}(0:T)\right)\right) = \underset{\boldsymbol{u}_{0:60}}{argmin}\, J\left(G_{Max}\left(Sim\left(\boldsymbol{u}_{0:60}, \boldsymbol{x}^{init}, \boldsymbol{\theta}, \boldsymbol{f}, T\right)\right)\right). \#(Equation\ 39)$$

747

748 We numerically solved this optimization problem by following evolutionary programming.

749 Each individual has an oral glucose ingestion pattern. After initialization of the oral glucose

750 ingestion pattern of each individual, the algorithm outputs the oral glucose ingestion pattern that

751 minimizes the objective function value by repeating (i) the mutation steps through which a new

752 oral glucose ingestion pattern for each individual is proposed, and (ii) the selection steps

753 through which individual (and thus new pattern) are selected based on the value of the objective

754 function.

755 Denoting the total number of individuals as N, the n^{th} individual of the oral glucose

756 ingestion pattern $\boldsymbol{u}_{0:60}$ as $\boldsymbol{u}_n$, and simplifying the objective function as $J(\boldsymbol{u}_n)$, the algorithm

is as follows:

1. (***Initialization***) For each individual $n = 1, \ldots, N$, $\boldsymbol{u}_n$ is initialized and $\boldsymbol{u}_n$ that minimizes $J(\boldsymbol{u}_n)$ is stored as $\boldsymbol{u}^*$.
2. Repeat the following procedure (a)–(c) K times
   a. (***Mutation***) For each individual $(n = 1, \ldots, N)$, copy and mutate $\boldsymbol{u}_n$ to generate a new individual $\boldsymbol{u}'_n$. Update $\boldsymbol{u}^*$ as $\boldsymbol{u}^* \leftarrow \boldsymbol{u}'_n$ if $J(\boldsymbol{u}^*) > J(\boldsymbol{u}'_n)$.
   b. (***Selection* 1**) For each of $2N$ individuals that consist of the original individuals and the new individuals generated at (a), obtain the evaluation value by the following procedure.
      i. Select an individual sequentially as $\boldsymbol{u}_m$.
      ii. Select an M individuals randomly except for $\boldsymbol{u}_m$ (duplication possible) as u_{m_i} $(i = 1, \ldots, M)$.
      iii. Obtain the evaluation value defined by the number of u_{m_i} with $J(\boldsymbol{u}_{m_i}) > J(\boldsymbol{u}_m)$.
   c. (***Selection* 2**) Sort the individuals in order of the evaluation value, and the top N individuals are selected and used in the next step.

3. Output $\boldsymbol{u}^*$.

In terms of evolutionary programming, step 1 is initialization, step 2-a is mutation, and steps 2-b and 2-c are selection. Because the intersection of oral glucose ingestion patterns is complicated by the constraint of 50 g total ingestion dose, this algorithm does not include intersection.

Details of initialization and mutation are as follows: In initialization, to avoid bias of an initial value, N individuals consist of an individual with a 50 g bolus ingestion, an individual with 1 g ingestion at 0 min and the remaining 49 g ingestion at 60 min, and other random patterns. The random pattern was generated by distributing 49 g glucose randomly with equal probability at each time point and the remaining 1 g ingestion at 0 min. For the mutation, a new oral glucose ingestion pattern was suggested by repeating operations that transfer 1 g of glucose from one time point to another randomly. Specific operations are as follows.

1. Subtract 1 g of glucose at time 0 min
2. Repeat the following procedure (a) and (b) L times
    a. Randomly select the source and destination time points of glucose with equal probability.
    b. If the ingestion glucose at the source time point contains more than 1 g, transfer 1 g of

789 glucose from the source time point to the destination time point.

790 3. Add 1 g of glucose at time 0 min

791 In the deterministic numerical simulation Sim, we employed the Euler method with a time

792 step width of 0.001 [min] to shorten the calculation time. We also set T = 480 [min].

793 In the evolutionary programming, we set the number of individuals as $N = 500$, the number

794 of generation except initialization generation as $K = 500$, the number of transfers of glucose in

795 one mutation L to decrease from $L = 20$ by 1 every 25 generations, and the number of

796 individuals for calculation of evaluation value in selection as $M = N/5 = 100$. According to

797 this algorithm and these settings, we calculated the optimal ingestion pattern for 5 trials and

798 obtained the pattern that produced the smallest objective function. Note that we obtained the

799 same minimization pattern for each subject multiple times for multiple trials (all trials in subject

800 #1 and #2, 2 trials in subject #3).

801 ***B.4. Coarse Graining of Minimization Pattern***

802 We coarse-grained the minimization pattern into three periods: a start time (0 min) of the first

803 bolus ingestion, a continuous-like intermediate period, and an end time of the ingestion (Figure

804 5A, upper panel). The coarse-grained pattern was characterized by 5 parameters: the dose of

ingested glucose at 0 min u_0 [g], the start time of the intermediate period t_s [min], the duration of intermediate period Δt [min], the dose of ingested of glucose at the end time u_T [g], and the end time of the ingestion T [min]. Similar to Figure 4, t_s and Δt are multiples of 5 [min]. During the intermediate period (t_s to $t_s + \Delta t$), the dose of glucose, determined by subtracting u_0 and u_T from 50 g, is equally distributed every 5 minutes. The dose of ingestion during intermittent period is not limited to an integer. These are described as follows:

$$u_0 \in \{1, 2, \cdots, 50\}, \#(Equation\ 41)$$

$$u_T \in \{0, 1, \cdots, 50 - u_0\}, \#(Equation\ 42)$$

$$t_s \in \{5, 10, \cdots, 55\}, \#(Equation\ 43)$$

$$\Delta t \in \{0, \cdots, T - t_s - 5\}, \#(Equation\ 44)$$

and Equation 22 is replaced by

$$Glucose = \begin{cases} u_0/0.5, & 0 \le t < 0.5 \\ \dfrac{50 - u_0 - u_T}{\Delta t/5 + 1}/0.5, & t_i \le t < t_i + 0.5, t_i \in \{t_s, t_s + 5, \ldots, t_s + \Delta t\} \\ u_T/0.5, & T \le t < T + 0.5 \\ 0 & otherwise \end{cases}. \#(Equation\ 45)$$

Figure Legends

Figure 1. Study diagram.

Three subjects orally ingested glucose with 3 doses 75 g, 50 g and 25 g in 2 durations of bolus and 2 h-continuous ingestion. Time course data of blood glucose level, insulin level, C-peptide level, GIP level, and GLP-1 levels were obtained (Figure 2). We constructed models of the dynamics of these blood hormones and glucose for each subject as a forward problem (Figure 3). Using the models, we predicted the minimization pattern, the glucose ingestion pattern minimizing the peak value of blood glucose level for the ingestion of 50 g glucose within 60 min as an inverse problem, and validated the pattern experimentally (Figure 4). To explore key parameters of the minimization pattern, we performed coarse-grain analysis (Figure 5).

Figure 2. Time course data of blood glucose level and blood hormones in subject #1 by glucose ingestion.

(A, B) Blood glucose. (C, D) insulin. (E, F) C peptide. (G, H) intact GIP. (I, J) intact GLP-1. (A, C, E, G, I) Bolus ingestion. (B, D, F, H, J) 2 h-continuous ingestion. The doses are indicated in panel A.

Figure 3. The blood glucose control model.

(A) Model diagram. The letters in the circle indicate the variables of the model, the arrows indicate the flow of molecules, the red lines indicate activation, and the blue line indicates suppression (see STAR Methods B.1). The best fitting models for subjects #1 and #3 lack the GLP1 components. (B) Temporal patterns of hormones. The blue lines indicate the temporal patterns of simulations, and the red circles indicate the time course data of experiments. The dose and ingestion pattern are indicated at the top.

Figure 4. Optimal Patterns minimizing the peak value of blood glucose level.

(A) Minimization patterns for glucose ingestion that minimize the peak value of blood glucose level in subject #1, #2, and #3. (B) Temporal patterns of blood glucose simulated from ingestion of glucose according to the minimization pattern (red line), bolus ingestion (black solid line), or 1 h-continuous ingestion (black broken line). The peak values achieved for each ingestion

pattern are marked with dashed horizontal lines. (C) Time course data of blood glucose level by the ingestion of the minimization pattern (red line and points and square symbols), the bolus ingestion (black solid line and open circles), and 1 h-continuous (black broken line and x symbols). The peak values achieved for each ingestion pattern are marked with dashed horizontal lines.

Figure 5. Coarse-grain analysis of minimization pattern.

(A) Coarse-grained minimization pattern characterized by 5 parameters, the dose of ingested glucose at 0 min u_0, the start time of the intermediate period t_s, the duration of intermediate period Δt, the dose of ingested of glucose at the end time u_T, and the end time of the ingestion T (B) T-dependency of u_0, u_{60}, t_s, and Δt that realize the minimum value of peak value of blood glucose level for each subject..

Tables

Table 1. Equations in the ordinary differential equation models. The estimated parameters are the 18 parameters of $k_2, k_3, k_4, k_5, k_6, k_7, k_8, k_{10}, K_2, K_4, K_6, K_8, K_{11}, V, a, b, c,$ and d. Simulations started from the models with initial concentrations of $GIP(0), GLP1(0), G(0), I(0), CP,$ and $X(0)$. Using the variables, and assuming $Duod_G, Ra_{GutG}, GIP, GLP1, G, I, X,$ and CP are at steady state before ingestion, other initial conditions and parameters, $Ingest_G(0), Ra_{GutG}(0), k_9, k_{11}, k_{12}, k_{13}, GIP_B$, and $GLP1_B$, were determined by estimated parameters and initial values (Equations 23–30).

Equation	Definition
$\frac{dIntest_G}{dt} = v_1 - v_6, \#$(Equation Error! Book	Change in glucose amount in the intestine $Intest_G$ [g] over time
$\frac{dGIP}{dt} = v_2 + v_3, \#$(Equation Error! Bookm	Change in GIP concentration *GIP* [pM] over time
$\frac{dGLP1}{dt} = v_4 + v_5, \#$(Equation Error! Bookm	Change in GLP-1 concentration $GLP1$ [pM] concentration over time
$\frac{dRa_{GutG}}{dt} = v_6 - v_7, \#$(Equation Error! Book	Change in the rate of appearance of ingested glucose in the blood Ra_{GutG} [g/min]
$\frac{dG}{dt} = \frac{v_7}{V} + v_8 - v_9, \#$(Equation Error! Bookr	Change in blood glucose concentration G [mg/dL]; constant V converts ingested glucose amount into blood glucose concentration
$\frac{dI}{dt} = v_{10} - v_{11}, \#$(Equation Error! Bookma	Change in blood insulin concentration I [pM]
$\frac{dCP}{dt} = v_{10} - v_{12}, \#$(Equation Error! Bookm	Change in C-peptide concentration CP [pM]
$\frac{dX}{dt} = \frac{v_{11}}{k_{11}} - v_{13}, \#$(Equation Error! Bookma	Change in insulin concentration acting at target

	organs to regulate glucose concentration in the blood X [dimensionless]
$v_1 = Glucose, \#$(Equation Error! Bookma	Influx of ingested glucose into the intestine
$v_2 = \frac{k_2\ Intest_G}{K_2 + Intest_G}, \#$(Equation Error! Bookr	Ingested glucose-dependent secretion of GIP by the intestine
$v_3 = k_3\ (GIP_B - GIP), \#$(Equation Error! Bool	Absorption of GIP by the intestine and entry into the blood
$v_4 = \frac{k_4\ Intest_G}{K_4 + Intest_G}, \#$(Equation Error! Bookr	Ingested glucose-dependent secretion of GLP-1 by the intestine
$v_5 = k_5\ (GLP1_B - GLP1), \#$(Equation Error! Bo	Absorption of GLP-1 by the intestine and entry into the blood
$v_6 = \frac{k_6\ Intest_G}{K_6 + Intest_G}, \#$(Equation Error! Bookr	Absorption of ingested glucose from intestine into rate of appearance for continuous ingestion
$v_7 = k_7\ Ra_{GutG}, \#$(Equation Error! Bookma	Absorption of ingested glucose from rate of appearance into blood for bolus
$v_8 = \frac{k_8}{K_8 + X}, \#$(Equation Error! Bookmar	Flow of glucose produced by the liver into the blood
$v_9 = k_9\ G\ X, \#$(Equation Error! Bookmar	Glucose uptake from the blood into the periphery
$v_{10} = k_{10}(G + a\ GIP + b\ G\ GIP + c\ GLP1$ (Equation Error! Bookmark not d	Insulin secretion; a, independent action of GIP; b, cooperative action of GIP with glucose; c, independent action

	of GLP-1; d, cooperative action of GLP-1 and glucose
$v_{11} = \frac{k_{11}\, I}{K_{11} + I}$, #(Equation Error! Bookma	Flow of insulin into target organs
$v_{12} = k_{12}\, CP$, #(Equation Error! Bookmar	Inactivation of C-peptide
$v_{13} = k_{13}\, X$, #(Equation Error! Bookmar	Binding of insulin to target cells

865

Table 2. Properties of the models. The ODE model has 16 parameters. The roles of the incretins in each subject's best fitting full model are shown, along with the predicted peak of blood glucose concentrations achieved with the minimization. The values of the parameters of the coarse-grained models that produced the peak value of blood glucose level for each subject are indicated.

	ODE model	Course-grained minimization pattern
Subject #1	Cooperative effect of GIP with glucose Minimization pattern: peak value of blood glucose level = 173.95 mg/dL	$u_0 = 17$ [g] $u_{60} = 24$ [g] $t_s = 30$ [min] $\Delta t = 0$ [min] Peak value of blood glucose level = 174.07 mg/dL
Subject #2	Independent effect of GIP Cooperative effect of GLP-1 with glucose Minimization pattern: peak value of blood glucose level = 112.36 mg/dL	$u_0 = 7$ [g] $u_{60} = 34$ [g] $t_s = 20$ [min] $\Delta t = 20$ [min] Peak value of blood glucose level = 112.43 mg/dL
Subject #3	Cooperative effect of GIP with glucose Minimization pattern: peak value of blood glucose level = 125.14 mg/dL	$u_0 = 6$ [g] $u_{60} = 31$ [g] $t_s = 20$ [min] $\Delta t = 30$ [min] Peak value of blood glucose level = 125.75 mg/dL

Figure 1

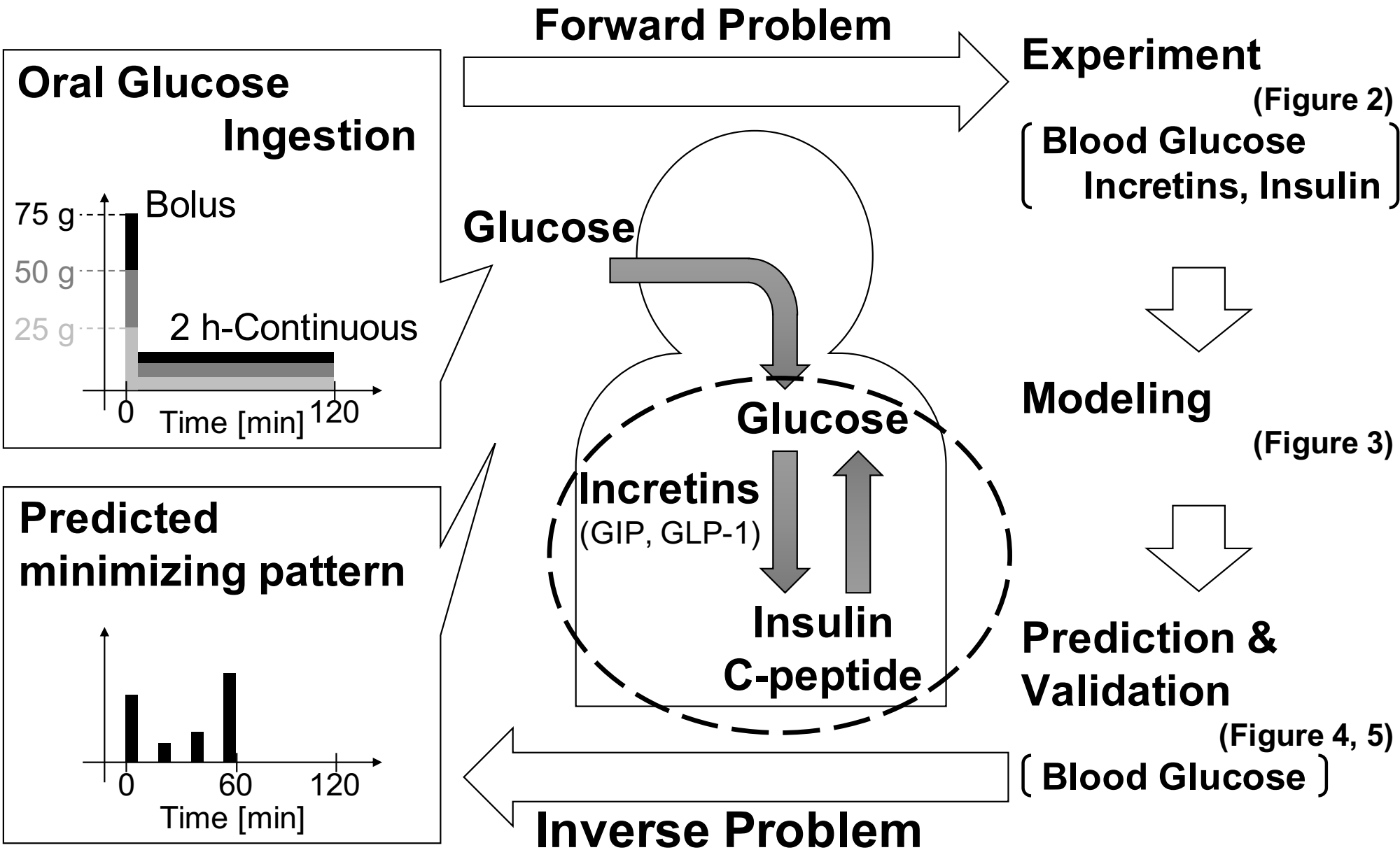
Forward Problem
Experiment
(Figure 2)
Blood Glucose
Incretins, Insulin
Oral Glucose Ingestion
75 g
50 g
25 g
Bolus
2 h-Continuous
0
Time [min]
120
Glucose
Glucose
Incretins
(GIP, GLP-1)
Insulin
C-peptide
Modeling
(Figure 3)
Predicted minimizing pattern
0
60
120
Time [min]
Prediction & Validation
(Figure 4, 5)
Blood Glucose
Inverse Problem

Figure 2

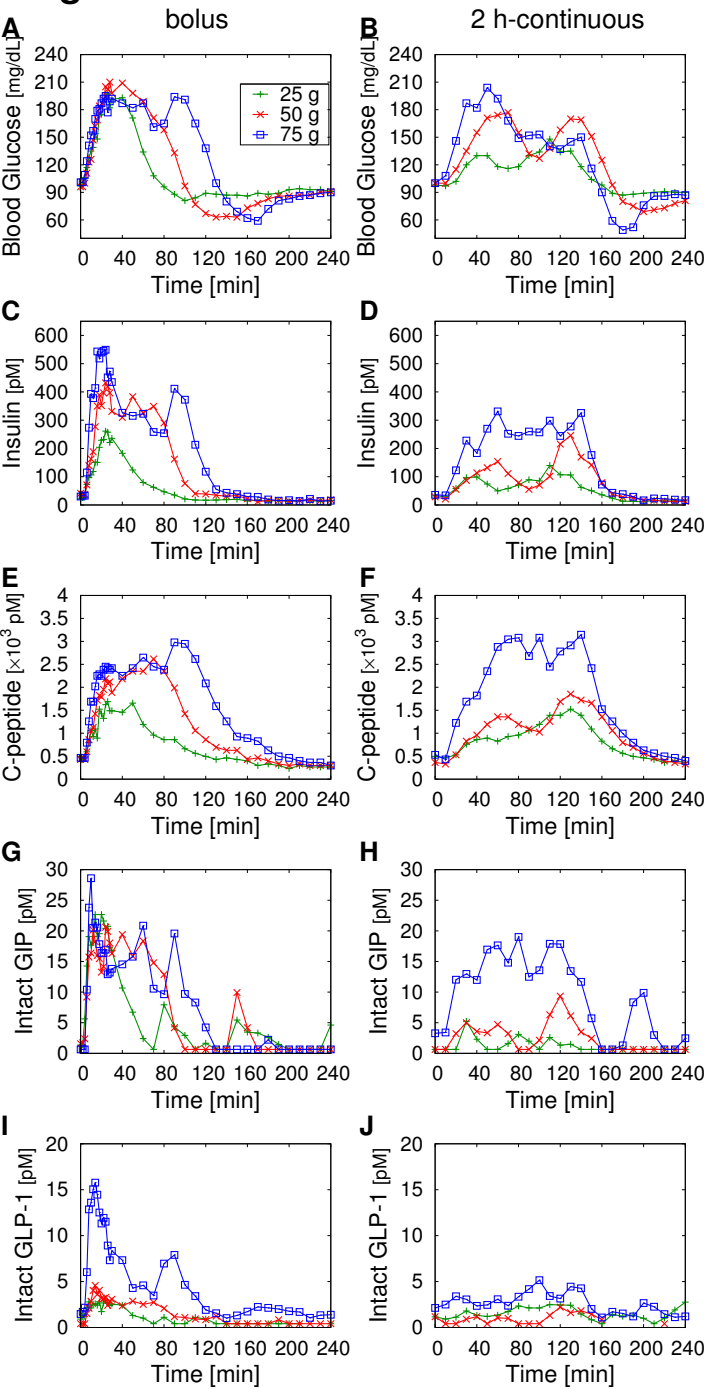
bolus
2 h-continuous
A
B
C
D
E
F
G
H
I
J
Blood Glucose [mg/dL]
Insulin [pM]
C-peptide [×10^3 pM]
Intact GIP [pM]
Intact GLP-1 [pM]
Time [min]
25 g
50 g
75 g

Figure 3

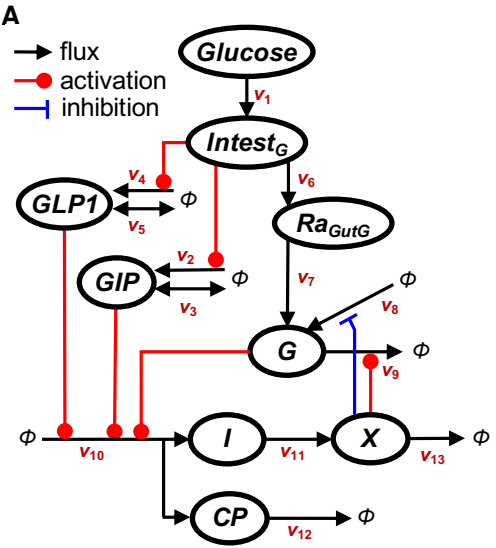
A
flux
activation
inhibition
Glucose
v_1
$Intest_G$
v_4
v_5
v_6
GLP1
Ra_{GutG}
v_2
v_3
v_7
v_8
GIP
G
v_9
v_{10}
I
v_{11}
X
v_{13}
CP
v_{12}
Φ

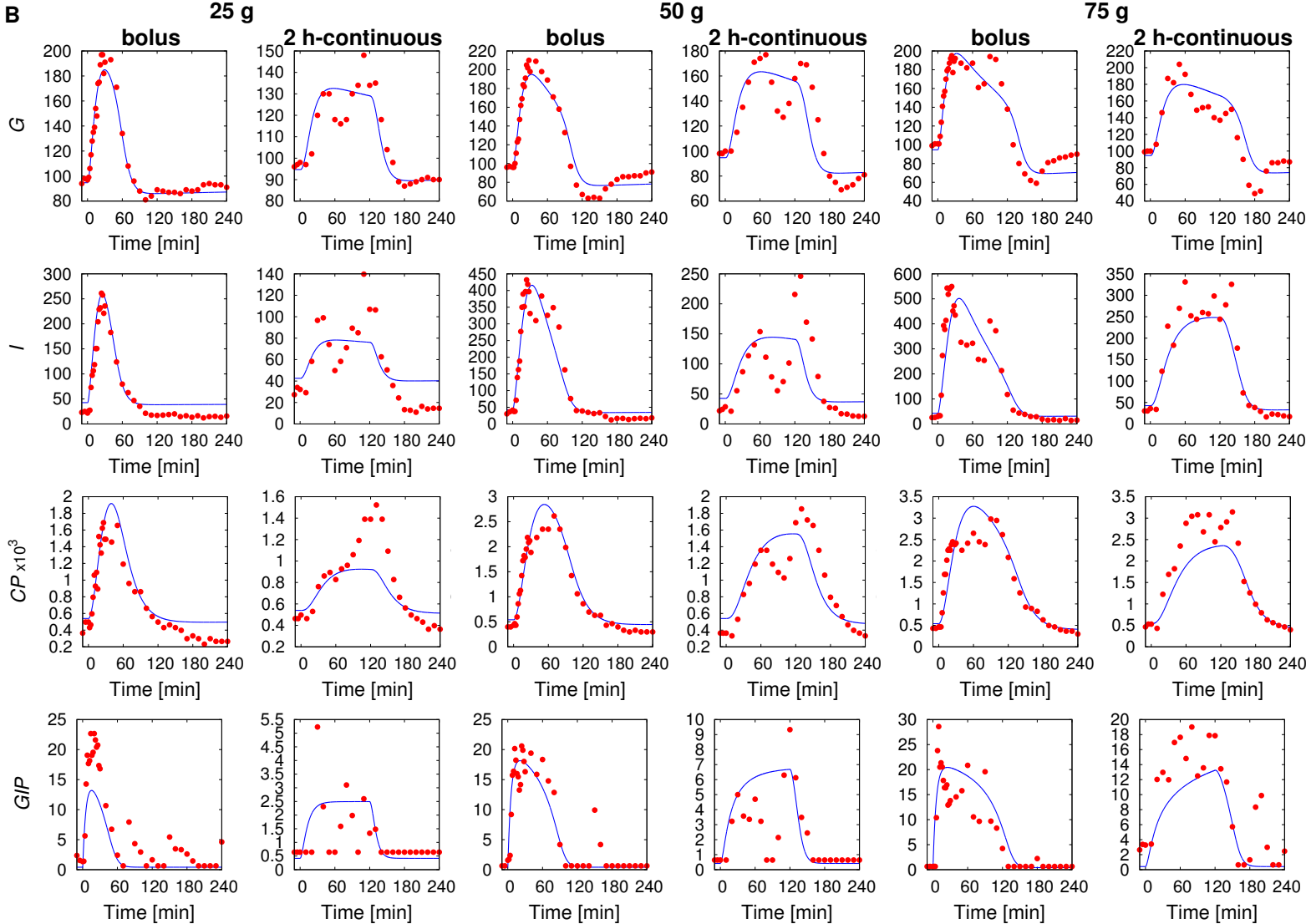
B
25 g
50 g
75 g
bolus
2 h-continuous
G
I
CP x10^3
GIP
Time [min]

Figure 4

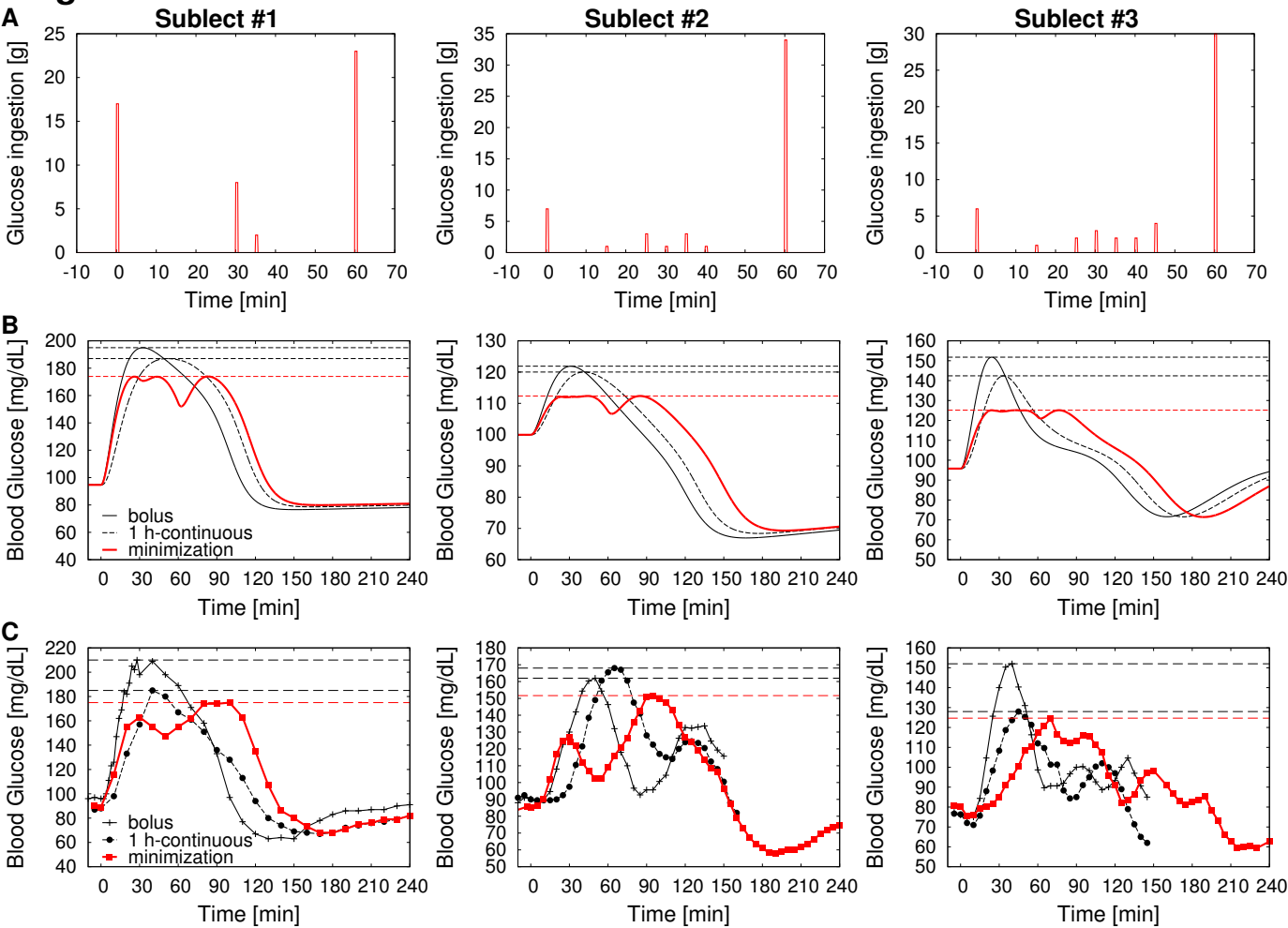
A
Sublect #1
Sublect #2
Sublect #3
Glucose ingestion [g]
Time [min]
B
Blood Glucose [mg/dL]
bolus
1 h-continuous
minimization
Time [min]
C
Blood Glucose [mg/dL]
bolus
1 h-continuous
minimization
Time [min]

Figure 5

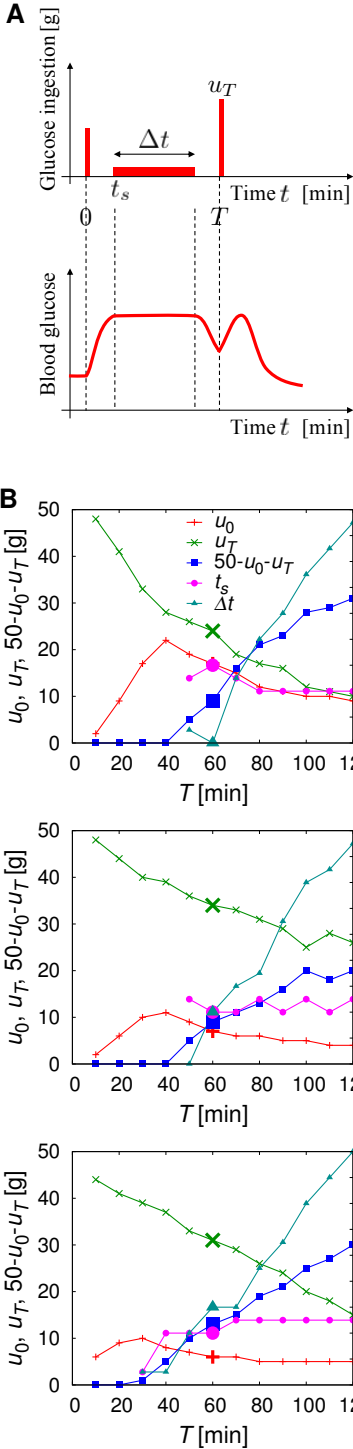
A
Glucose ingestion [g]
u_T
Δt
t_s
Time t [min]
0
T
Blood glucose
Time t [min]
B
u_0
u_T
50-u_0-u_T
t_s
Δt
u_0, u_T, 50-u_0-u_T [g]
t_s, Δt [min]
T [min]